JOURNAL OF MATERIALS SCIENCE 27 (1992) 6365–6370

Demonstration of nuclear magnetic resonance imaging for void detection in carbon-fibre reinforced polymer composites, and comparison with ultrasound methods

P. JEZZARD*, C. J. WIGGINS, T. A. CARPENTER, L. D. HALL§
Herchel Smith Laboratory for Medicinal Chemistry, University of Cambridge School of Clinical Medicine, University Forvie Site, Robinson Way, Cambridge CB2 2PZ, UK

J. A. BARNES
ICI Composites Inc., 2055 East Technology Circle, Tempe, Arizona 85284, USA

P. JACKSON‡§, N. J. CLAYDEN
ICI plc, Wilton Materials Research Centre, PO Box 90, Wilton, Middlesbrough, Cleveland TS6 8JE, UK

Nuclear magnetic resonance imaging has been used as a method of void detection in carbon-fibre reinforced polymer composites. This is accomplished by observation of signal from water molecules which have ingressed into surface-connected defect regions within the polymer composite. Problems associated with the conductivity of these samples are discussed, along with methods of overcoming those difficulties.

1. Introduction

During the past two decades nuclear magnetic resonance (NMR) imaging has become an important diagnostic medical tool, and much research effort has been invested in this area [1, 2]. Recently, a few groups have turned their attention to the many non-medical applications which exist, which include: oil/water mapping in rock cores [3, 4], void detection in amorphous polymers [5–7], studies of the spatial dependence of bulk polymerization reactions [8], studies of wood [9], and applications of NMR imaging in the food industry [10]. We have also demonstrated the potential use of NMR imaging in the detection of voids within polymer composites [11, 12], in particular in carbon-fibre reinforced polymer composites [13]. During a subsequent extensive survey of carbon-fibre reinforced polymer composites, we have compared the results of NMR imaging studies with those of ultrasound studies, and now present representative images here. In addition, we have discovered that there are circumstances under which it is not possible to obtain NMR images of carbon-fibre reinforced polymer composites; in this paper we discuss those circumstances and describe ways in which an NMR image may nevertheless be obtained.

Carbon-fibre reinforced polymer composites are becoming increasingly important in the manufacture of high-performance products, including applications in the aviation industry. Many of those products demand a defect-free material to cope with the high-stress regimes which may be encountered in their use, and consequently several techniques for defect detection in these materials have been developed. However, standard methods for the analysis of carbon-fibre polymer composites are limited in their application: by low transmission in the case of X-ray radiography, and by a restriction to flat laminate plates in the case of ultrasonic methods. We have previously demonstrated how NMR imaging can be used to provide a map of the spatial distribution of surface-connected voids by collecting signal from water which has ingressed into those voids [13]; that technique need not be restricted to flat sheets, and can provide a fully quantitative map of the distribution of ingressed water.

1.1. NMR imaging

In an NMR imaging experiment a spatial map of the concentration of the magnetic nucleus of interest is obtained (the hydrogen nucleus in the experiments described here). This is achieved by placing the sample in a strong static magnetic field (the $\boldsymbol{B}_0$ field), thereby causing it to acquire a magnetization vector in the

* *Present address*: Laboratory for Cardiac Energetics, National Heart Blood and Lung Institute, National Institutes of Health, Bethesda, Maryland, USA.
‡ *Present address*: ICI Specialities, Specialities Research Centre, PO Box 42, Blackley, Manchester M9 3DA, UK.
§ Authors to whom correspondence should be addressed.

0022–2461

direction of the static field. By application of a pulse of radio-frequency energy of the correct frequency and duration the magnetization vector can be tipped such that it is perpendicular to the static field, causing it to precess about $\boldsymbol{B}_0$ and inducing an alternating current in the NMR probe placed around the sample. In a homogeneous static field the characteristic resonance frequency of the precession about $\boldsymbol{B}_0$ is identical for nuclei in all parts of the sample, and is given by $\omega = \gamma B_0$ where γ is the gyromagnetic ratio for the nucleus of interest. In an NMR imaging experiment the value of the homogeneous $\boldsymbol{B}_0$ field is made spatially dependent by application of a magnetic field gradient. In that way the local resonance frequency of the spins uniquely determines a plane in the sample, resulting in an induced NMR signal which contains a range of frequencies corresponding to the spatial extent of the sample, the intensity of which is weighted by the local spin density in each of the elemental planes; Fourier transformation of that signal thus results in a one-dimensional spatial profile of the sample.

A variety of techniques exist for generating a two- or three-dimensional NMR image of the sample, such as reconstruction from a set of 1D profiles obtained at different gradient angles [14], and reconstruction by 2D and 3D Fourier imaging [15]. In the experiments presented here the 2D and 3D spin warp imaging sequences of Edelstein *et al.* [15] are used, in which a spatially encoded spin-echo is formed a time TE after the initial excitation of the sample. Spin–spin relaxation puts an upper limit on the echo time, TE, which can be used, since the NMR signal at the time of the spin-echo decays according to $S(t) \propto \exp(-TE/T_2)$, where T_2 is the charcteristic spin–spin relaxation time of the spin system. In most medical applications the T_2 of the mobile water and lipid is typically several hundred milliseconds, which allows plenty of time for the hardware manipulations to be carried out to enable the NMR signal to be spatially encoded. In many materials science applications, however, the T_2 value of the sample lies in the range 10 μs–10 ms, which places much more stringent timing and switching requirements on the hardware necessary to generate an image. In a solid polymer composite, the polymer matrix itself generally has a T_2 value less than 100 μs, which makes the direct imaging of solid polymer composites very difficult (and impossible for samples of dimension > 2 cm using current state-of-the-art hardware). A more realistic approach is to introduce a mobile liquid (having a T_2 value of $\gg 100$ μs) into the voids, thereby enabling the simpler, slower-switching, liquid-state imaging techniques to be used. In such cases, signal from the solid polymer does not appear in the final image because it will have decayed to zero intensity during the acquisition time.

2. Experimental procedure

All NMR imaging experiments presented here were performed using a Bruker Biospec I spectrometer attached to a 31 cm horizontal-bore superconducting magnet operating at 2 T (83.7 MHz proton frequency) and using a series of home-made probes. The transverse field gradients (x and y) are provided by a standard Golay design [16], and the longitudinal gradient (z) by a Maxwell pair design, each driven by pairs of Tecron 7570 audio amplifiers operating in push–pull configuration, providing a maximum field gradient of $30\ \mathrm{mT/m^{-1}}$ and a gradient switch-on/switch-off time of 100 μs. These values are much better than those normally encountered in medical NMR imaging, and reflect the demands of the different regime presented by materials imaging.

Each composite sample was boiled overnight in water before commencing the NMR imaging experiment; this allows water to penetrate into any surface-connected voids present in the sample and provides the mobile liquid which is subsequently imaged. Loss of liquid during imaging is minimized by wrapping the sample in cellulose film. Care must be taken when comparing the measured weight uptake of water during the boiling process with the amount of water observed in the NMR images [17]. This is because the water taken up by the polymer composite can exist in two states: interstitial water contained in void spaces, generally having a T_2 value of many milliseconds, and bound water, which is strongly associated with the polymer matrix and has a very short T_2 value (typically < 100 μs). In the NMR images presented here only signal from the interstitial water is observed, since the T_2 relaxation time of the bound water is much shorter than the spin-echo time used. In fact, the polymer matrices we have studied are ultra-high density, and so the absolute amount of bound water which diffuses into them is quite small.

The ultrasound scans were obtained at 5 MHz, and the sample and ultrasound transmitter/receiver were both immersed in a water bath for maximum coupling. Two-dimensional ultrasound maps were acquired of flat plates of polymer composite in times ranging from 10 to 30 min, depending on sample size. These ultrasound maps show the reflected energy, $I(x, y)$, from a thin beam of ultrasonic waves; the higher the attenuation of the reflected beam the more voiding is present in the sample. In this way a qualitative map of the degree of voiding can be obtained, though the technique is restricted to flat plates because of spurious scattering occurring in samples of a more complex shape.

3. Results

3.1. Void detection in flat composite sheets

In order to compare qualitatively the level of quality-control testing achievable by NMR imaging with that of a standard technique we have obtained NMR images and ultrasound maps of the same pieces of both laminated carbon-fibre reinforced thermoplastic composite and laminated carbon-fibre reinforced thermoset composite, in each of which serious flexural and impact damage had been deliberately induced; that damage resulted in considerable delamination which is largely undetectable by simple visual inspection. The first sample studied was a carbon-fibre reinforced thermoplastic polymer composite measuring

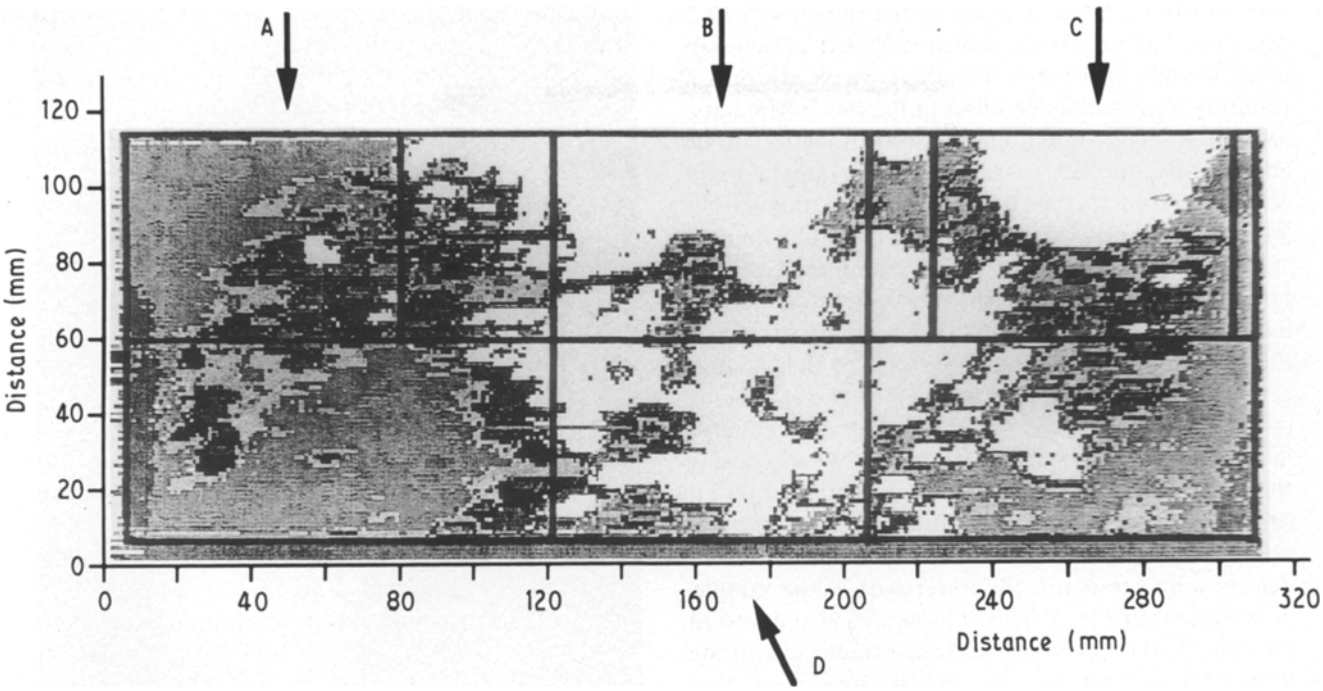

Figure 1 Map of ultrasound attenuation versus position for a sample of laminated carbon-fibre reinforced poly(ether ether ketone) measuring 30 cm × 11 cm × 0.6 cm. Regions of defect show up bright on the scan. Also marked on the diagram are the four plates A–D which were cut from the large sheet for NMR analysis.

30 cm × 11 cm × 0.6 cm, which was manufactured using a standard autoclave forming technique; the sample consisted of 32 laminate sheets in a (0°, 90°, − 45°, + 45°) lay-up. A conventional "C-scan" ultrasound map [18] of the sample was obtained, giving a map of the attenuation of the reflected ultrasound beam as a function of position in the x–y plane, with no z resolution. Fig. 1 shows the ultrasound scan obtained of the entire sample, with regions of defect showing up as light areas (increased reflected-beam attenuation). Clearly a large portion of this sample has been damaged, and this sample would have been discarded on the basis of that examination.

The sample was then cut into the sections marked on Fig. 1, and these sections were boiled overnight in water. The sections marked A, B, C and D, measuring 85 mm × 55 mm (the largest size that will currently fit inside our probe, though a larger probe is being developed), were then imaged individually. Since the T_2 relaxation time of the magnetization originating from the polymer is so short, only magnetization originating from the ingressed water molecules is observed in the NMR images (Fig. 2). A version of the spin-wrap imaging sequence [15] without slice-selection was used with a spin-echo time of 5.6 ms. This echo time is considerably shorter than the echo times commonly used in medical imaging, and is used because of the short spin–spin (T_2) relaxation time of the ingressed water which governs the time allowable between initial excitation of the magnetization and the spin-echo. We have found that the T_2 value of water contained within voids in a composite is often substantially shorter than the T_2 value of the bulk water used to boil the sample (in the case of this sample the values were 13 and 1100 ms, respectively). This difference is caused by a combination of restricted molecular motion within the voids leading to inefficient averaging of line-broadening mechanisms and diffusion of the water through large susceptibility gradients within the voids; both of these effects lead to a shorter T_2 value.

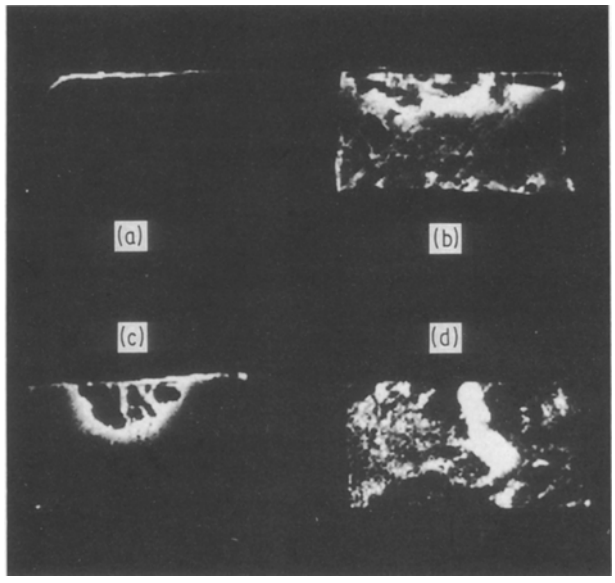

Figure 2 A–D show 128 × 128 pixel images of the corresponding sections taken from the sample shown in Fig. 1. Water ingressed into the voided regions shows up bright in the NMR images. A spin-echo time of 5.6 ms was used in conjunction with a 4 s scan repeat time, giving a total imaging time of 20 min per image, which included a two-step phase cycling routine.

The NMR images presented in Fig. 2 show a clear correlation with the ultrasound map shown in Fig. 1, demonstrating that for surface-connected void detection the NMR method provides a comparable tool to

the ultrasound method. Each image shown in Fig. 2 was acquired in 20 min, which included a two-step phase cycling process to eliminate image distortion resulting from a baseline offset in the raw NMR data. As well as images of flat plates, NMR imaging can be additionally applied to samples exhibiting a more complex geometry, as demonstrated in our earlier letter [13], whereas the ultrasound method cannot.

The second sample studied was a laminated carbon-fibre reinforced epoxy (thermoset) polymer composite measuring 14 cm × 10 cm × 0.8 cm, again fabricated in the shape of a flat plate. In the case of this sample, severe impact damage was inflicted on the sample by dropping a 0.2 kg mass on to the centre of the large face of the laminate plate from a height of 1 m, causing the central region of the sample to splinter. Ultrasound analysis of this sample shows that in addition to severe damage to the centre of the sample, further defects were present in the lower part of the sample, as is evident in Fig. 3. This sample was also cut to fit into the NMR probe, yielding a sample measuring 9 cm × 5.5 cm × 0.8 cm. An NMR image of that sample, showing a 2 mm thick slice taken from the centre of a three-dimensional data-set, is shown in Fig. 4. This image was accomplished using a 128 × 128 pixel spin-warp sequence to produce a square image in the plane of the laminate sheets, whilst additionally using a 16-step phase encoding gradient in the thin dimension to produce a 128 × 128 × 16 voxel image following three-dimensional Fourier transformation. This enables individual slices from the sample to be inspected, allowing depth resolution of sample defects to be achieved. The image shown in Fig. 4 corresponds to a 2 mm slice through the centre of the laminate plate, and clearly shows a defective area in the lower part of the sample with preferential uptake of water along the fibre directions. An increase in the number of phase encode steps in the slice direction would allow an improved z (depth) resolution to be attained, although at the expense of an increased data acquisition time. The image shown in Fig. 4 was acquired using a 7 ms echo time, a 1 s scan-repeat time, and was signal-averaged twice, giving an overall data acquisition time of 35 min for the full data-set.

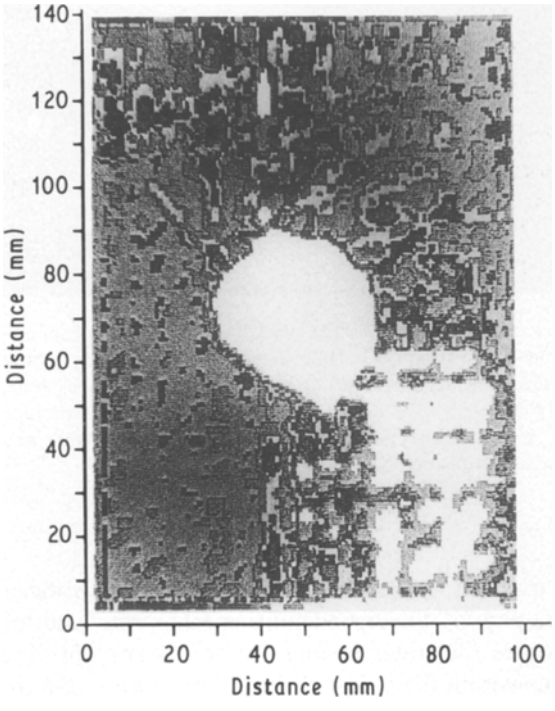

Figure 3 Map of ultrasound attenuation versus position for a sample of laminated carbon-fibre reinforced epoxy thermoset polymer composite measuring 14 cm × 10 cm × 0.8 cm. The sheet had been impact-damaged by dropping a weight on to the centre of the plate.

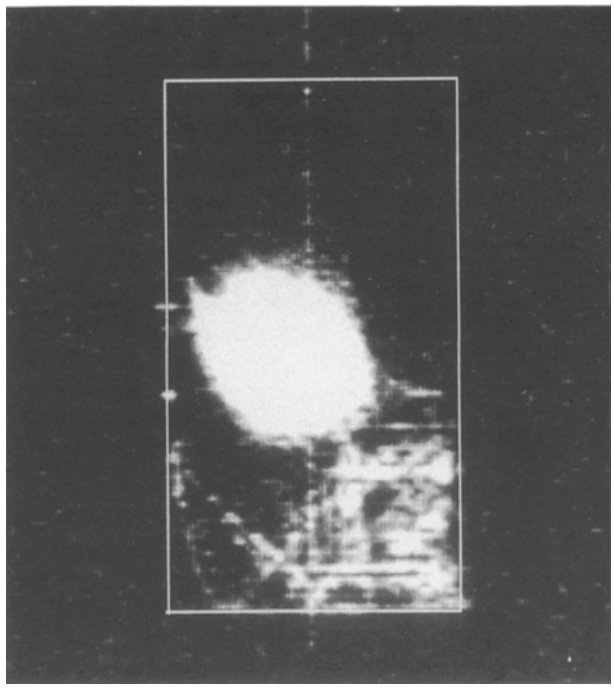

Figure 4 128 × 128 pixel image of the distribution of ingressed water in the thermoset polymer composite shown in Fig. 3. The image is taken from a 128 × 128 × 16 voxel data-set, acquired using 16 phase encode steps in the slice direction. Spin-echo time = 7 ms, scan-repeat time = 1 s. The outline of the sample is also shown.

3.2. Sample conductivity effects

In the course of our studies we found that there are circumstances where NMR images of laminated carbon-fibre polymer composites cannot be obtained straightforwardly; this occurs in cases where the plane of the laminate sheets is perpendicular to the direction of the radio-frequency magnetic field ($\boldsymbol{B}_1$). This problem arises because the carbon fibres form a conducting mesh which acts to screen the radio-frequency field within the coil; this problem does not occur in non-conductive samples, such as glass-fibre reinforced polymer composites. Two orientations of the laminate sheets with respect to the $\boldsymbol{B}_1$ field are shown in Fig. 5. In Fig. 5a the laminate sheets are perpendicular to the $\boldsymbol{B}_1$ field, a configuration resulting in no signal being detected from water-filled voids within the composite. In Fig. 5b the laminate sheets are parallel with the $\boldsymbol{B}_1$ field, and this orientation allows images of internal water distribution to be generated.

The implication of these observations is that in the case of laminated carbon-fibre reinforced polymer composites the sample must be aligned in the probe so

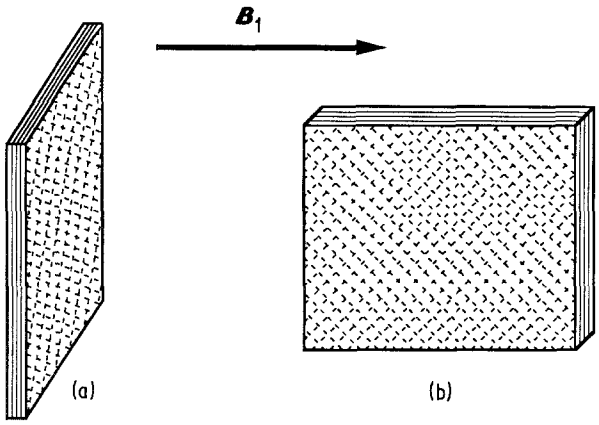

Figure 5 (a) Perpendicular and (b) parallel orientations of the laminate planes of a carbon-fibre reinforced polymer composite with respect to the direction of the B_1 field. In the case of (a) no signal from the ingressed water can be detected.

as to ensure that the B_1 field direction is parallel to the local laminate plane direction throughout the sample. This is possible for many samples of interest, for example in flat plaques where two laminate sheets are heat-welded together to form a butt joint, or where orthogonal bending of the laminate sheets is introduced. The anisotropy in the NMR response of laminated carbon-fibre polymer composites is clearly demonstrated in the NMR response to a simple 90° excitation pulse, which shows no signal for a sample with its laminate plane perpendicular to the B_1 field direction, and full signal for a sample with its laminate plane parallel to the B_1 field.

3.3. Void detection in more complex shapes

In order to demonstrate how the NMR imaging technique may be used in circumstances in which conventional ultrasound techniques would fail, we have studied a number of samples with geometries other than flat laminate plates. One such example is shown in Fig. 6. This sample consists of three separate components of identical carbon-fibre reinforced thermoplastic polymer composite: one flat multi-laminate base plate, and two L-shaped multi-laminate plates, all heat-welded together in the form shown in the centre of Fig. 6. The two L-sections measure 50 mm in length and are 1 mm thick, with a leg length of 20 mm; the flat plate measures 50 mm in length by 40 mm width and is 2 mm thick. The data were collected as a $64 \times 64 \times 64$ voxel three-dimensional image using a 3D spin-warp sequence, as described in section 3.1 above, yielding a pixel resolution of 1 mm. A two-step phase cycling routine was used to signal-average the data, resulting in a total data acquisition time of 2.5 h.

The data were then transferred to a Sun 4/150 workstation incorporating a TAAC applications accelerator unit. A volume-rendered 3D movie loop of the image data was constructed using the standard Sun VOXVU and A2BITMOVIE programs. Those processes calculate the ray-casted view of the 3D image data-set from 32 directions, angularly separated by 11.25° about the long axis of the sample. Those

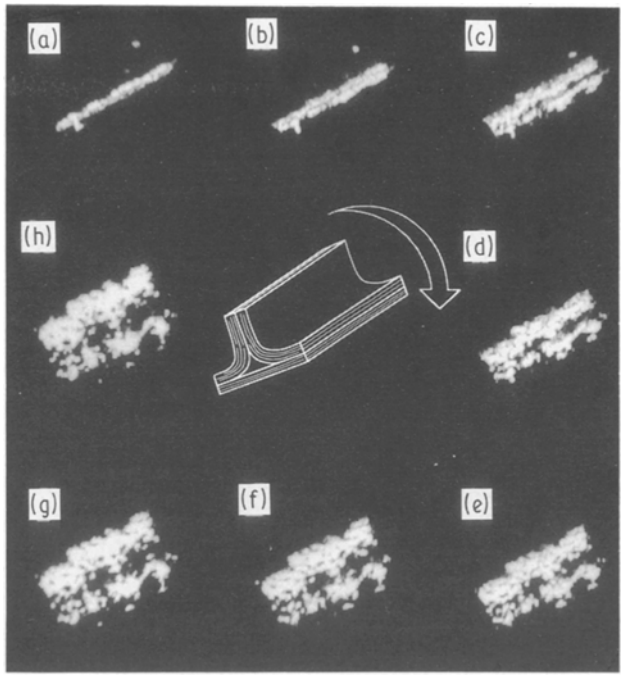

Figure 6 Selected snapshots from the video movie of a three-component T-weld sample as the sample is rotated through 90°. It is evident from the images that the heat-welding of the two curved laminate sheets on to the flat laminate plane is unsatisfactory. Spin-echo time = 8 ms, scan-repeat time = 1 s.

views can then be displayed in quick succession using the TAAC unit, resulting in a rotating 3D display of the data. This means of viewing the data, rather than the more standard slice-by-slice means, is particularly suited to applications involving "unfamiliar" samples, where very little prior knowledge of the form of the data exists (this differs from many medical applications where the anatomy of the brain, for example, is well known by the viewer and has many familiar features to aid spatial location). Fig. 6 shows eight views from the movie loop of the T-weld sample, obtained as the data-set is rotated through 90°. It is evident that the majority of the ingressed water lies in a plane parallel with the flat base plate, and in fact resides in void spaces between the L-shaped sections and the base plate, thereby demonstrating a "bad" weld joint between these components.

4. Conclusion

In conclusion, we have generated defect maps from samples of carbon-fibre reinforced polymer composite using both standard ultrasonic methods and NMR imaging methods. Both techniques yield similar two-dimensional information which delineate the distribution of defects within flat laminated sheets. However, additionally, NMR imaging methods can straightforwardly be extended to obtain three-dimensional information and can be used to study more complex shapes. NMR imaging has the further capability of "zooming in" to study a smaller region of interest with improved resolution [20], and of obtaining quantitative results for void sizes. We have also discovered that an NMR signal cannot be generated from regions

of a carbon-fibre reinforced polymer composite sample where the laminate sheets are perpendicular to the direction of the radio-frequency field within the NMR probe. This problem can be ameliorated either by orienting the sample with the laminations parallel to the radio-frequency field direction, or, if this is not possible for the whole sample, by obtaining image data-sets at various orientations and then combining the information at those orientations to generate a complete map of the water distribution. In the case of glass-fibre reinforced polymer composites we have found no such anisotropy in the NMR response from a laminated material. NMR imaging can also be used to observe the production of polymer composites by observing signal from the heated, and therefore more mobile, polymer matrix itself.

Acknowledgements

The authors wish to thank Dr Herchel Smith for an endowment (T.A.C. and L.D.H.) and for a research scholarship (P. Jezzard). We also thank Dr N. J. Herrod and Dr A. J. de Crespigny at the Herchel Smith Laboratory for provision of image display software.

References

1. P. MANSFIELD and P. G. MORRIS, "NMR Imaging in Biomedicine", Supplement 2 of in "Advances in Magnetic Resonance", edited by J. S. Waugh (Academic, New York, 1982).
2. P. G. MORRIS, "Nuclear Magnetic Resonance Imaging in Medicine and Biology" (Oxford University Press, New York, 1986).
3. W. A. EDELSTEIN, H. J. VINEGAR, P. N. TUTUNJIAN, P. B. ROEMER and O. M. MUELLER, S.P.E. paper 18272, Proceedings of the 63rd Annual Technical Conference and Exhibition, Houston, Texas, October, 1988.
4. M. A. HORSFIELD, C. HALL and L. D. HALL, *J. Magn. Resonance* **87** (1990) 319.
5. T. A. CARPENTER, L. D. HALL and P. JEZZARD, *ibid.* **84** (1989) 383.
6. A. G. WEBB, P. JEZZARD, L. D. HALL and S. NG, *Polym. Commun.* **30** (1989) 593.
7. P. JEZZARD, T. A. CARPENTER, L. D. HALL, P. JACKSON and N. J. CLAYDEN, *ibid.* **32** (1991) 74.
8. P. JACKSON, N. J. CLAYDEN, N. J. WALTON, T. A. CARPENTER, L. D. HALL and P. JEZZARD, *Polym. Int.* **24** (1991) 139.
9. L. D. HALL, V. RAJANAYAGAM, W. A. STEWART, P. STEINER and S. CHOW, *Can. J. Forest Res.* **16** (1986) 684.
10. S. L. DUCE, T. A. CARPENTER and L. D. HALL, *Lebensm.-Wiss. Technol.* **23** (1990) 545.
11. P. JACKSON, N. J. CLAYDEN, J. A. BARNES, T. A. CARPENTER, L. D. HALL and P. JEZZARD, in Proceedings of 36th International SAMPE Symposium, San Diego, April 1991, (SAMPE, California, 1991).
12. *Idem.*, in Proceedings of 12th International SAMPE (Europe) Conference, Maastricht, May 1991 (Elsevier, 1991).
13. P. JACKSON, J. A. BARNES, N. J. CLAYDEN, T. A. CARPENTER, L. D. HALL and P. JEZZARD, *J. Mater. Sci. Lett.* **9** (1990) 1165.
14. R. A. BROOKS and G. DI CHIRO, *Phys. Med. Biol.* **21** (1976) 689.
15. W. A. EDELSTEIN, J. M. S. HUTCHISON, G. JOHNSON and T. REDPATH, *ibid.* **25** (1980) 771.
16. M. J. E. GOLAY, *Rev. Sci. Instum.* **29** (1958) 313.
17. P. JACKSON, *J. Adhesion* **33** (1990) 1.
18. J. KRAUTKRÄMER and H. KRAUTKRÄMER, "Ultrasonic Testing of Materials" (Springer, Berlin, 1969).
19. P. JACKSON, *J. Mater. Sci.* **27** (1992) 1302.
20. A. J. S. DE CRESPIGNY, T. A. CARPENTER and L. D. HALL, *J. Magn. Reson.* **88** (1990) 406.

Received 11 July 1991
and accepted 17 February 1992